TECHNICAL REPORT: CALCULATING AGRICULTURAL VALUE

The Changing Wealth of Nations 2021

Managing Assets for the Future

WORLD BANK GROUP

THE CHANGING WEALTH OF NATIONS 2021

Managing Assets for the Future

TECHNICAL REPORT

CALCULATING AGRICULTURAL VALUE

WORLD BANK GROUP

1818 H Street, NW
Washington, DC 20433
Telephone: 202-473-1000
Internet: www.worldbank.org

Changing Wealth of Nations

Calculating agricultural value

James S. Gerber
Paul West
Ethan Butler
Deepak Ray
Justin Johnson

December 4, 2020

INSTITUTE ON THE
ENVIRONMENT
UNIVERSITY OF MINNESOTA
Driven to Discover℠

This work was part of World Bank contract number **7192822 "Analysis in support of the Global Program for Sustainability"**

Overview

This report describes work carried out by a team of researchers at the University of Minnesota to improve calculations of agricultural wealth which comprise an important component of the *Changing Wealth of Nations* (CWON) analysis. This report contains a description of contract deliverables, detailed methods, and proposals for future improvements for calculation of agricultural value.

The main text provides a brief review of the previous and new methodology for calculating the value of agriculture. The primary advancement presented here that the net annual growth pattern is estimated annually for ten major crops. Further, the analysis was done at the sub-national level and then aggregated to country- and regional-scale values. Following the main text, a series of appendices provide more details on the methods of calculating: current and future yields (Appendix A), slopes on agricultural land (Appendix B), land degradation (Appendix C), and crop area under future scenarios (Appendix D). In addition, we include brief summaries of recommended improvements (Appendix E), and Lessons Learned (Appendix F).

This work was part of World Bank contract number **7192822 "Analysis in support of the Global Program for Sustainability"**

Approach to calculation of Changing Wealth of Nations

1. Prior methodology

The first edition of CWON calculated the value of cropland as the present value of rents generated by cropland over its lifetime. The value is calculated in 2 steps:

Step 1. Annual resource rents for a given year, $TR_{c,t}$, are the sum of the rents, $R_{c,k,t}$, for each crop, k, in each country, c, in a given year, t. Rents are the product of price (p), quantity(q) produced and a rental rate parameter (for regions, not country specific):

$$TR_{c,t} = \sum_{k=1}^{n} R_{c,k,t}$$

where

$$R_{c,k,t} = \left(p_{c,k,t} \times q_{c,k,t} \times a_{Reg}\right)$$

for

c = roughly 150 countries
k = 1,…,n for number of crops covered by FAO
t = 1995 to 2018, or latest year available
a_{Reg} = average rental rate across all crops in a region, REG = 1,…,14
Reg, as defined by the Evenson and Fuglie study used for rental rates. The rental rate is the ratio of (price – cost) / price. The rental rate is not given a *t* subscript because it is assumed to be constant over time.

In each year, p x q = FAO's Gross Value of Production (GVP).
(As noted in the CWON methodology documentation, *p* and *q* are 5-year lagged averages, not annual values.)

How Step 1 is implemented for CWON: Because we do not have separate rental rates for each crop, k, or for every year, t, the equations can be implemented using FAO data for Gross Value of Production (GVP):

$$TR_{c,t} = GVP_{c,t} \times \alpha_{Reg}$$

Step 2. Asset value, $V_{c,\tau}$ is then calculated as the discounted sum of total rents over the lifetime, T, with a discount rate, r, of 4%; the core accounts assumed an infinite time horizon in prior calculations, but this is revised to 100 years**.**

Asset value, V, is then calculated as the discounted total rents over time for each country:

$$V_{c,\tau} = \sum_{t=\tau}^{T} TR_{c,t} \times (1+g_d)^t \Big/ (1+r)^t$$

This assumes that total rents grow annually at the rate, g_d

g_d = 1.94% for low- and middle-income countries, and
g_d = 0.97% for high-income countries; all annual growth rates are constant over time

The net growth parameter, g, can result from any combination of several factors
higher crop yield rates, a change to higher value crop mix, or an expansion of cropping area, net of any land degradation; The growth rate in prior calculations was not crop specific.
The parameter, g, here is revised, incorporating changes across crops and over time.

2. New Methodology

The methods used for this report build upon the approach used in the previous CWON report. The major advancement is that here growth is calculated annually for each of 10 major crops (it was previously assumed constant across time and crops). This improvement was made possible using a sub-national time series of crop yield and area (Ray et al. 2019).

2.1 The basic 2-step approach remains the same.

Annual resource rents are calculated in the same way using the same parameters and variables. FAO data are used for price (p) and quantity (q); the same regional average rental rate is used

$$TR_{c,t} = \sum_{k=1}^{n} R_{c,k,t}$$ where $$R_{c,k,t} = \left(q_{c,k,t} \times p_{c,k,t} \times a_{Reg}\right)$$	Equation 1

Variables are defined as in Section 1, above

Asset value, $V_{c,\tau}$ is calculated as the discounted sum of total rents over the lifetime, T=100 years, with a discount rate, r, of 4%, but the annual net growth is now estimated annually for each of 10 major crops, k, in each country, c. Growth can vary over time (with a limit on unconstrained growth) for each of the 10 crops (in contrast to the earlier approach which assumed continuous growth).

Going forward, instead of using growth rate g we introduce a growth factor γ. This change is motivated by the fact that the growth factor can vary from year to year, rendering the term $(1+g)^t$ difficult to generalize. If we introduce the growth factor γ, it is easy to relate to the $(1+g)^t$ term for the case of constant $(1+g)^t$:

$$Increase\ in\ yield\ in\ year\ t = (1+g)^t = \gamma_t$$

For the case where yearly growth factor is not constant, we have

$$Increase\ in\ yield\ in\ year\ t = \prod_{i=1}^{t}(1+g_i)^{t} = \gamma_t$$

Although we continue to use the term 'growth' for the parameter, γ, it is possible that there is actually a decline in the change of yield over time and γ could be less than 1. Three separate impacts on growth are estimated: crop yield trend due to technical improvements, $\gamma_{c,k,t}^{yt}$, climate change impact on yields, $\gamma_{c,k,t}^{CC}$, and land degradation impacts on yield, $\gamma_{c,k,t}^{LD}$, which can result from multiple causes such as soil erosion, salination, etc.

crop technical yield trend (+ or -), $\gamma_{c,k,t}^{yt}$
climate change impact (+ or -), $\gamma_{c,k,t}^{CC}$
land degradation impact (-), $\gamma_{c,k,t}^{LD}$

$\gamma_{c,k,t}^{Y} = \gamma_{c,k,t}^{yt}\gamma_{c,k,t}^{CC}\gamma_{c,k,t}^{LD}$	Equation 2

Estimation of γ starts with estimation of annual crop yield growth due to technical change, γ^{yt}, which is then adjusted for the impacts on yield of climate change and land degradation. These factors are described in later sections.

The individual yield growth factors, $\gamma_{c,k,t}^{Y}$, are calculated for each of the 10 major crops and are then aggregated to country and regional average yield growth rates and applied to FAO's Gross Value of Production (GVP), discussed below. The estimation of crop-specific yield growth rates $\gamma_{c,k,t}^{Y}$ is discussed in Appendix A: Yield Calculations. Here we only discuss how to aggregate crop level estimates to national and regional average growth rates.

2.2 National yield growth rates: country averages vs regional averages

The CWON asset valuation method requires a *national level* average annual production growth factor that can be applied to FAO's Gross Value of Production (GVP). The production growth factor is the product of the yield growth factor $\gamma_{c,t}^{Y}$, and an area growth factor. In the present analysis, cropped area is held constant over time (so the area growth factor = 1.0).

The present analysis calculates yield growth factors for a total of 10 crops, which together constitute some fraction F of each country's agricultural production value. If that fraction F is 100%, the national yield growth can be calculated as the annual weighted yield growth factor for each crop, $\gamma_{c,k,t}^{Y}$, with weights supplied by the value share of production for each crop. This approach would be reasonably accurate even when the 10 crops account for less than 100% of

GVP, but still comprise a 'substantial' share. At the other extreme, a country might not produce any of the 10 crops covered in the estimation. Rules for estimating national yield curves are needed in such countries.

CWON often uses 'regional' averages for gap filling or when the country-level information is not sufficient to provide a reasonable estimate. To determine whether country or regional average yields should be used, we examine how much the 10 crops--mostly cereals, grains and oil crops—account for a country's GVP.
The 10 crops represent a large share of *land area* under cultivation in many countries, but account for a smaller share of the *value* of agricultural production, GVP. Over the period 2011-2016 the average share of the 10 crops in GVP ranges from 0 to 100% across countries, and averages 42% at the global level. The 10 crops accounted for at least 50% of GVP in only 43 countries. If we applied a strict country-data approach to calculate national average yields from the 10 crops, countries where none of the 10 crops are produced would have zero yield growth. In countries where the 10 crops accounted for as little as 1% of GVP, the national yield would be determined by that 1%. Given the limited share of the 10 crops in many countries, we will calculate regional average growth rates to apply at the country level. This approach is less than ideal but still an improvement over the estimates in earlier versions of CWON.

In practice, crop-weighted growth-rate parameters are calculated and presented at both the country and regional levels. To guide the decision about which parameter to use, a calculation is made and presented for every country of the fraction of 2016 values for the 10 crops to total GVP, and a decision can be made globally or regionally on what minimum value of the value ratio is required to use for the country-specific growth rate.

2.3 Aggregation of yield growth factors to the regional level

Regional average yield growth factor $\gamma^{Y}_{Reg,t}$, is derived from country-level estimates, weighted by the value of the 10 crops for which yield growth is estimated. This is done in two steps: first calculating national weighted average yield growth factors, $\gamma^{Y}_{c,t}$ then calculating regional averages with country weights for the 10 crops over the *n* countries in each region. National level weights for each crop are calculated based on the 10-year best-fit of time series of agricultural value obtained from FAO.[1] See Appendix E for a discussion of the units of agricultural value. The two-step approach preserves information at the country level for later analysis.

Step 1. National average yield growth:

Average yield growth at the national level is calculated as the average of yield growth rates for each crop weighted by that crop's value of production (Equation 3).

[1] Price time-series are obtained and processed for both Gross Production Value (constant 2004-2006 1000 I$) and Gross Production Value (constant 2004-2006 million US$) so as to minimize impact of missing FAO data. We used 2004-2006 USD for all cases except if price data wasn't available from FAO in units of 2004-2006 USD.

$\gamma_{c,t}^{y} = \sum_{k=1}^{10} \gamma_{c,k,t}^{y} \times {p_{c,k,t} q_{c,k,t}}/{GVP_{c,t}^{C10}}$ where, $GVP_{c,t}^{C10}$ is the sum of production across the 10 crops, k=1…10. $GVP_{c,t}^{C10} = \sum_{k=1}^{10} p_{c,k,t} \times q_{c,k,t}$	Equation 3

Note there is a modification carried out to Equation 3 (see Appendix E) for the case where value of production data is reported in incommensurate units within a country for different crops.

Step 2. Regional average yield growth:

$$\gamma_{Reg,t}^{Y} = \sum_{c=1}^{n} \gamma_{c,t}^{Y} \times {GVP_{c,t}^{C10}}/{GVP_{Reg,t}^{C10}}$$

where

$$GVP_{Reg,t}^{C10} = \sum_{c=1}^{n} GVP_{c,t}^{C10}$$

2.3 Calculation of Value of Agricultural land.

Based on Equation 1, and the growth rates aggregated either to the regional or country scale ($\gamma_{Reg,t}^{Y}$ or $\gamma_{c,t}^{Y}$ respectively), value of agricultural land is calculated as the discounted total rents, TR, with annual growth (relative to year 2018) of $\gamma_{Reg,t}^{Y}$ or $\gamma_{c,t}^{Y}$, over a lifetime of 100 years.

Regionally aggregated of growth rates:

$$V_{c,\tau} = \sum_{t=\tau}^{\tau+100} TR_{c,t} \times \gamma_{Reg,t}^{Y} / (1+r)^{t}$$

Country-aggregated growth rates:

$$V_{c,\tau} = \sum_{t=\tau}^{\tau+100} TR_{c,t} \times \gamma_{c,t}^{Y} / (1+r)^{t}$$

Data used in calculations

Yield and Area data

Yield and harvested area data for major crops were from a data set recently developed by the UMN team (Ray et al. 2019). The data set was constructed using crop statistics from 1974-2012 across ~20,000 political units globally. The ten crops in the data set—barley, cassava, maize, oil palm, rapeseed, rice, sorghum, soybean, sugarcane, and wheat—account for ~83% of global kilocalorie production from all croplands.

To extend the data to 2018, we used FAO's national level production statistics to *perturb* our most recent sub-national statistics in our data set so that the new national totals for both area and yield match the data on FAOStat. In other words, we assume that subnational distribution of crop production remains constant when we extend the data set to more recent years. For the ten major crops, we perturbed a smoothed version of the 2010 sub-national data (This smooth version is constructed as the average of 2008-2012 so as to minimize the impact of weather-induced yield aberrations).

We note there is a temptation to extrapolate year 2000 data for other crops (beyond the 10 crops for which we had circa 2010 data) in this manner. However, we tested this approach and found that the reliability of this nearly 2-decade extrapolation unacceptable. We hope that future work will allow us to constrain the extrapolation with satellite date, thus resulting in an acceptable dataset with more crops.

Deliverables

Output tables:
For each of 156 countries,

four .csv tables have been delivered via dropbox

```
combinedgrowthfactors_FRA_SSP2_RCP45RevF.csv
combinedgrowthfactors_FRA_SSP3_RCP70RevF.csv
combinedgrowthfactors_FRA_SSP1_RCP26RevF.csv
historicalyieldandprice_FRARevB.csv
```

thirty figures have been delivered via dropbox

```
YieldtrendsFRA_France_barley_SSP_1_RCP_2_6.png
YieldtrendsFRA_France_cassava_SSP_1_RCP_2_6.png
YieldtrendsFRA_France_maize_SSP_1_RCP_2_6.png
YieldtrendsFRA_France_oilpalm_SSP_1_RCP_2_6.png
YieldtrendsFRA_France_rapeseed_SSP_1_RCP_2_6.png
YieldtrendsFRA_France_rice_SSP_1_RCP_2_6.png
YieldtrendsFRA_France_sorghum_SSP_1_RCP_2_6.png
YieldtrendsFRA_France_soybean_SSP_1_RCP_2_6.png
YieldtrendsFRA_France_sugarcane_SSP_1_RCP_2_6.png
YieldtrendsFRA_France_wheat_SSP_1_RCP_2_6.png
```

YieldtrendsFRA_France_barley_SSP_2_RCP_4_5.png
YieldtrendsFRA_France_cassava_SSP_2_RCP_4_5.png
YieldtrendsFRA_France_maize_SSP_2_RCP_4_5.png
YieldtrendsFRA_France_oilpalm_SSP_2_RCP_4_5.png
YieldtrendsFRA_France_rapeseed_SSP_2_RCP_4_5.png
YieldtrendsFRA_France_rice_SSP_2_RCP_4_5.png
YieldtrendsFRA_France_sorghum_SSP_2_RCP_4_5.png
YieldtrendsFRA_France_soybean_SSP_2_RCP_4_5.png
YieldtrendsFRA_France_sugarcane_SSP_2_RCP_4_5.png
YieldtrendsFRA_France_wheat_SSP_2_RCP_4_5.png
YieldtrendsFRA_France_barley_SSP_3_RCP_7_0.png
YieldtrendsFRA_France_cassava_SSP_3_RCP_7_0.png
YieldtrendsFRA_France_maize_SSP_3_RCP_7_0.png
YieldtrendsFRA_France_oilpalm_SSP_3_RCP_7_0.png
YieldtrendsFRA_France_rapeseed_SSP_3_RCP_7_0.png
YieldtrendsFRA_France_rice_SSP_3_RCP_7_0.png
YieldtrendsFRA_France_sorghum_SSP_3_RCP_7_0.png
YieldtrendsFRA_France_soybean_SSP_3_RCP_7_0.png
YieldtrendsFRA_France_sugarcane_SSP_3_RCP_7_0.png
YieldtrendsFRA_France_wheat_SSP_3_RCP_7_0.png

Appendix A: Yield calculations

Overview

Future yields for 10 major crops were estimated through a several step process. First, current yield ceilings (attainable, not theoretical or experimental yields) were estimated using a quantile regression model with inputs of climate, soils, irrigation, and topography. Second, a future yield ceiling was defined by assuming that yield ceiling trends will continue to 2050 (or sooner for regions with identified potential for land degradation.) Next, impacts of climate change are allowed to modify the time series of yield ceiling. Because climate and land degradation are currently impacting yields, yields observed over 30 years are extrapolated until the curve intersects the yield ceiling curve or 0 yield.

Figure 1 below shows the key steps behind calculations of yield. The scattered "x" values represent empirically observed maize yields for Australia. The red smooth curve represents a yield ceiling in the absence of land degradation and climate change. This yield ceiling is calculated from the 95th quantile of many thousands of empirical yield observations from all countries (corrected for biophysical factors). The yield ceiling shows linear growth over the period 2000-2018, reflecting growth in yields and the constraints of the model. This yield ceiling continues to grow until 2050, at which point it is held constant. Land degradation is applied as a further limit to allowed yield growth, this effectively causes the yield ceiling to be reached before 2050. The purple * represents the smoothed yield in 2018 … this is calculated as a least-squares best fit of the previous 30 years of data. The green curve represents the extension of the Australian yield data (allowing for continued technical growth). This curve continues until it hits the yield ceiling modified for land degradation. Then, climate change acts as a multiplier of the yield ceiling time series across the entire time series from 2019 to 2100.

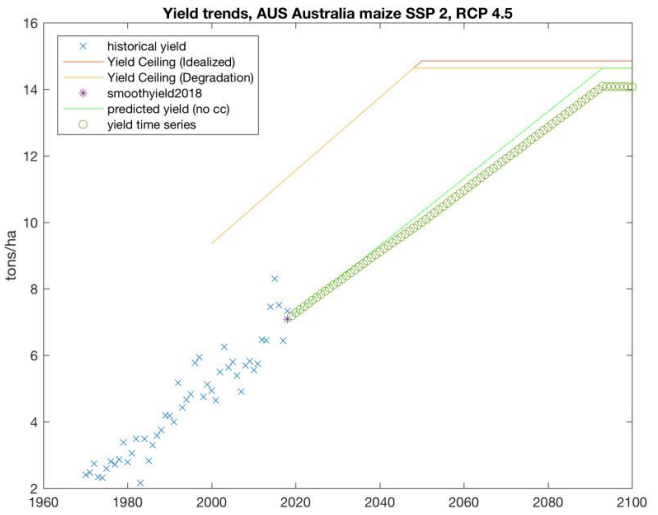

Figure 1 Components of yield calculation

There is another special case which obtains when the reported yield exceeds the calculated yield ceiling (since the yield ceiling is the 95th percentile yield, it is expected that this will happen in some cases). When this obtains, yield is allowed to continue to grow from the reported yield value, following technical trends which are the smaller of the following two slopes (country-specific technical trend in yield (i.e. fit to previous 30 years of data) or slope of the attainable yield trend from the quantile regression. An example is below for maize in Israel. Israel historically has reported maize yields far above regional (and global) averages – so any empirically modeled yield based on a reasonable number of parameters will be less than reported yields, as is the case here.

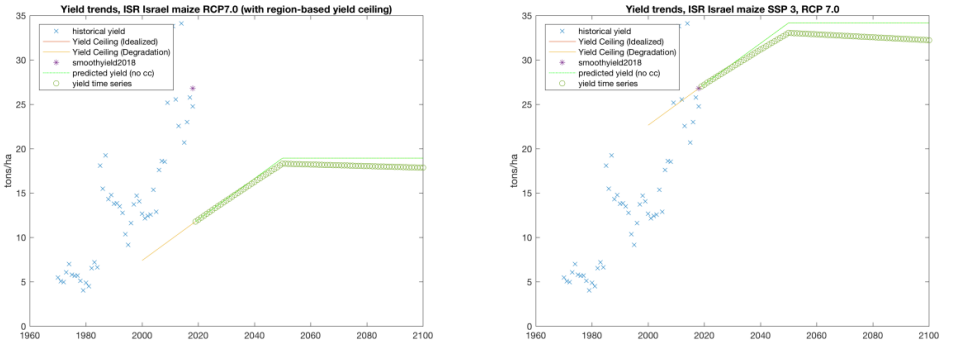

Figure 2 Components of yield calculation in the case where reported yields exceed calculated yield ceiling. In Figure a, the reported yield is much greater than the calculated yield ceiling. Figure b shows the resolution of this case … predicted future yield grows from the reported yield time series, although the slope is limited to the calculated slope of yield ceiling.

Prediction of future yield ceilings

Future yield ceiling in the absence of climate change and land degradation (baseline)

The yield ceiling is allowed to increase over time, subject to an exogenous constraint: The World Bank team recommended that the growth in the yield ceiling not be allowed to extend for more than 30 years past the present day (i.e. to 2050.)

The 2018 yield model was quantified using a quantile regression model that includes a set of two temperature variables, two precipitation variables, three soil variables, and one topography variable The two temperature terms are growing degree days (GDD) and extreme degree days (EDD). GDD is a commonly used agronomic term that estimates crop development, calculated as the sum of daily temperature values over a base value. In contrast, EDD is a measure of extreme temperatures that are detrimental to yield. Like temperature, precipitation is included through both mean annual precipitation (MAP) and an estimate of its distribution over the growing season (Precipitation Concentration Index (PCI)). We include the interaction of mean annual precipitation with all terms as water availability may alleviate stress from excess temperature, mild temperatures are of little benefit to a moisture starved crop, and more concentrated precipitation may provide less usable water.

Three soil variables are included: soil organic carbon (SOC), pH (pH), and available water capacity (AWC). SOC and pH are both proxies for soil fertility. SOC helps retain nutrients and pH affects whether or not the nutrients are available for the plant to access. AWC is a measure of how much water the soil can hold. Note that these variables are not completely independent. For example, sandy soils typically have lower SOC, pH, and AWC than silt loam soils do.

The topography variable is average slope of cropland within a census unit.

Irrigation is included as a management variable. It is also an interacted term with all climatic terms as it has a similar influence on yield as mean annual precipitation.

$$Y \sim C_i^0 + GDD + EDD + MAP + MAP^2 + PCI + GDD * MAP + EDD * MAP + PCI * MAP + IRR + IRR * GDD + IRR * EDD + IRR * MAP + IRR * PCI + AWC + SOC + PH + ESASlope + ESASlope^2 + t + t * C_i^1$$

Equation A1: Yield attainment model.

Variables are listed in Table A1 and crop-specific GDD values are in Table A2.

Table A1: Variables used in construction of yield attainment model

Variable	**Definition**	**Source**
C_i^0, C_i^1	Each region, C, will have an independent intercept C_i^0, as well as independent linear coefficients C_i^1. Regions based on Evenson and Fuglie (2010).	NA
GDD	Growing degree days, crop specific	World Clim V2.0 (Fick and Hijmans 2017)
EDD	Extreme degree days, maximum temperature greater than 30.	World Clim V2.0 (monthly current and future TMAX) (Fick and Hijmans 2017) + BEST (daily current TMAX) (Cowtan et al. 2019)
MAP	Mean annual precipitation	World Clim V2.0 (Fick and Hijmans 2017)
PCI	Precipitation concentration index	World Clim V2.0, Oliver, 1980 [(Oliver 2010)]
IRR	Fraction of area equipped for irrigation	(Portmann et al. 2010) (Siebert et al. 2015)
AWC	Available water capacity in upper 30cm of soil	SoilGrids250m / ISRIC (Hengl et al. 2017) [2019 update]
SOC	Soil Organic Carbon in upper 30 cm of soil	SoilGrids250m / ISRIC (Hengl et al. 2017) [2019 update]
pH	pH of soil, a good proxy for nutrient availability	SoilGrids250m / ISRIC (Hengl et al. 2017) [2019 update]
Slope	Average slope of agricultural parcels	ESA (European space agency land cover) 2015 data coupled with high-resolution slope data from HWSD/FAO
t	Year	NA

Table A2 Table of crop-specific Growing Degree Day (GDD) base temperatures

cropname	Base temperature (deg C)	Notes
'barley'	0	https://ndawn.ndsu.nodak.edu/help-barley-growing-degree-days.html
'cassava'	13	Computer Simulation of Cassava Growth, Mithra et al. 2018
'maize'	8	Mueller et al. 2012
'oilpalm'	20	Paterson et al. 2015

'rapeseed'	5	https://ndawn.ndsu.nodak.edu/help-canola-growing-degree-days.html
'rice'	5	Mueller et al. 2012
'sorghum'	10	Texas Cooperative Extension, Gerik et al,'Sorghum Growth and Development' http://hdl.handle.net/1969.1/87184
'soybean'	8	Mueller et al. 2012
'sugarcane'	12	Cuadra et al. 2011
'wheat'	0	Mueller et al. 2012

In this formulation EDD is calculated yearly, whereas all other variables are based on a climatology (30-year average).

EDD is calculated as follows for years where BEST (Berkeley Earth Surface Temperature) data is available:

- Calculate a daily BEST Tmax climatology over the same years used by WorldClim to calculate the WorldClim 2.1 climatology (1970-2000)
- Calculate a monthly BEST Tmax climatology by averaging over months [follow BEST conventions with regards to leapyear]
- Calculate a BEST Tmax anomaly by subtracting the BEST 1970-2000 Tmax monthly climatology from the annual BEST Tmax time series
- Disaggregate WorldClim temperature to make a daily timeseries (constant for each month)
- Add the BEST Tmax anomaly to the disaggregated WorldClim temperature. Downscale the BEST anomaly to WorldClim resolution (1 degree to 5 mins)
- Calculate EDD for each yearly subset of the resulting time series

Soil quality and area equipped for irrigation data were not calculated here. Rather, they were used directly from the data sets listed in Table 1.

The average slope of the 3-second agricultural pixels is the average slope of the 30 second pixels. Then, the agricultural slopes of the 30 second pixels are averaged up to the political unit (using a weighted average, where the weight is total agricultural area in 30 second pixel.) Slope on agricultural land is calculated at 300m by combining slope data from the Harmonized World Soils Database (Nachtergaele et al. 2009) and the ESA-Climate Change Initiative landcover data set (ESA 2017). An example slope calculation is in Appendix B Calculating slope on agricultural lands.

Model coefficients

See "CWON Final Tech Report Annex A _ Model specifications.docx"

Prediction of future yield

Predicted future yield is based on linear extrapolation of yield data based on the N years prior to (and including) 2018 where N is the number of points with defined yield and area values from FAO, where N is constrained to be at least 5 and no more than 30 years. This approach serves to predict yield into the future. Note that climate change and land degradation are known to be

impacting currently observed yields, so these extrapolated yields are not modified for climate change impacts until they intersect with the yield ceiling.

Impact of climate change on yield ceilings

The impact of climate change on yield ceilings is quantified using the above yield model with future climate estimates. More specifically, we use the predicted temperature and precipitation data from the Coupled Model Inter-comparison Project (CMIP). Climate change can have a negative or positive effect on yield.

Since the model is trained on a climatology based around the year 2000, by applying the model to a year 2050 climatology, we will be able to assess the relative difference in yield due to changes in climate from 2000 to 2050. We will apply this factor from year 2019 to 2050. We also carry out the same calculation for 2070, and apply that from 2051 to 2070, and extrapolate differences to 2100. In both cases, we assume that the impact of climate change is linear between the two modeled times (such as 2000 and 2050). Although this assumption is simplistic, temperature thresholds and non-linear responses to climate change are not well understood.

Future yields are calculated based on future climates predicted by each of 7 GCMs (Global Climate Models.) These 7 sets of future yields are averaged to produce a mean predicted yield at 2030, 2050, 2070, and 2100.

	Model Name	Full Name of Model	Institution	Citation	Publication link
1	MRI-ESM2-0	Meteorological Research Institute Earth System Model Version 2.0	Meteorological Research Institute, Tsukuba, Japan	Yukimoto et al., 2019	https://doi.org/10.2151/jmsj.2019-051
2	MIROC6	sixth version of the Model for Interdisciplinary Research on Climate	Research Center for Environmental Modeling and Application, Japan Agency for Marine-Earth Science and Technology	Tatebe et al., 2019	https://www.geosci-model-dev.net/12/2727/2019/
3	IPSL-CM6A-LR	Institut Pierre Simon Laplace	consortium of 9 research laboratories in France	Hourdin et al., 2019	https://agupubs.onlinelibrary.wiley.com/doi/full/10.1029/2019MS001666
4	CanESM5	Canadian Earth System Model version 5	Canadian Centre for Climate Modelling and Analysis, Environment and Climate Change	Swart et al., 2019	https://www.geosci-model-dev.net/12/4823/2019/
5	BCC-CSM2-MR	Beijing Climate Center Climate System Model	Beijing Climate Center, China Meteorological Administration, Beijing, China	Wu et al., 2016	https://www.geosci-model-dev.net/12/1573/2019/
6	CNRM-ESM2-1	Earth system model of CNRM	Centre National de Recherches Météorologiques	Séférian et al., 2016	https://www.geosci-model-dev.net/9/1423/2016/
7	CNRM-CM6-1	Centre National de Recherches Meteorologiques and Cerfacs	Université de Toulouse, Météo-France	Voldoire et al., 2019	https://agupubs.onlinelibrary.wiley.com/doi/full/10.1029/2019MS001683

For all future yield predictions, we assume that topography, soil properties, and the area equipped for irrigation remain constant (same values used in the 2018 yield ceiling calculations).

Impact of land degradation on yield ceilings

Land degradation also affects the yield ceiling. There are very few studies that define a relationship of yield response to land degradation. As such, we could not credibly include land degradation in the attainable yield model. Instead, we mapped three aspects of land degradation—soil erosion, salinization, and water depletion—and estimated their impact on yield based on the results from small-scale studies. Details are in Appendix C: Land degradation.

References

Cowtan, Kevin & National Center for Atmospheric Research Staff (Eds). Last modified 09 Sep 2019. The Climate Data Guide: Global surface temperatures: BEST: Berkeley Earth Surface Temperatures. Retrieved from https://climatedataguide.ucar.edu/climate-data/global-surface-temperatures-best-berkeley-earth-surface-temperatures.

Cuadra, S. V., Costa, M. H., Kucharik, C. J., da Rocha, H. R., Tatsch, J. D., Inman-Bamber, G., et al. (2011). A biophysical model of Sugarcane growth. *GCB Bioenergy*, *4*(1), 36–48. http://doi.org/10.1111/j.1757-1707.2011.01105.x

ESA. Land Cover CCI Product User Guide Version 2. Tech. Rep. (2017). Available at: maps.elie.ucl.ac.be/CCI/viewer/download/ESACCI-LC-Ph2-PUGv2_2.0.pdf

Evenson, R. E., & Fuglie, K. O. (2010). Technology capital: the price of admission to the growth club. *Journal of Productivity Analysis*, *33*(3), 173-190.

Fick, S.E. and Hijmans, R.J. (2017), WorldClim 2: new 1-km spatial resolution climate surfaces for global land areas. Int. J. Climatol, 37: 4302-4315. doi:10.1002/joc.5086

Hengl, T., Mendes de Jesus, J., Heuvelink, G. B. M., Ruiperez Gonzalez, M., Kilibarda, M., Blagotić, A., et al. (2017). SoilGrids250m: Global gridded soil information based on machine learning. *PLoS ONE*, *12*(2), e0169748. http://doi.org/10.1371/journal.pone.0169748.t004

Hijmans, R. J., Cassman, K. G., Cameron, S. E., Specht, J. E., Parra, J. L., Dobermann, A., et al. (2005). Very high resolution interpolated climate surfaces for global land areas. *International Journal of Climatology*, *25*(15), 1965–1978. http://doi.org/10.1002/joc.1276

Mithra, V. S. S., Radhakrishnan, A. R. S., & Lekshmanan, D. K. (2018). Computer Simulation of Cassava Growth. In *Cassava* (pp. 1–17). InTech. http://doi.org/10.5772/intechopen.71510

Mueller, N. D., Gerber, J. S., Johnston, M., Ray, D. K., Ramankutty, N., & Foley, J. A. (2012). Closing yield gaps through nutrient and water management. *Nature*, *490*(7419), 254–257. http://doi.org/10.1038/nature11420

Nachtergaele, F., van Velthuizen, H., FAO, L. V., Rome, Italy, 2009. (n.d.). Harmonized world soil database (version 1.1). *Library.Wur.Nl*

Oliver, J. E. (1980). Monthly precipitation distribution: a comparative index. *Prof. Geogr.* **32**, 300–309.

Paterson, R. R. M., Kumar, L., Taylor, S., & Lima, N. (2015). Future climate effects on suitability for growth of oil palms in Malaysia and Indonesia. *Scientific Reports*, 1–11. http://doi.org/10.1038/srep14457

Ray, DK, PC West, M Clark, JS Gerber, AV Prishchepov, S Chatterjee. 2019. Climate change likely already affects global food production. *PLOS ONE*. doi: 10.1371/journal.pone.0217148

Appendix B: Calculating slope on agricultural lands

ESA-CCI land cover data for 2015 was downloaded, and a mask of agricultural area aggregated to the 30 second scale (native resolution = 10 seconds) was computed. Agricultural area in each 30 second pixel is the sum of occurrence of agricultural classes 10, 11,12,20 plus the number of occurrences of the agricultural mosaic class 30 (multiplied by 0.75) plus the number of occurrences of the agricultural mosaic class 40 (multiplied by 0.25.)

Slope data was downloaded from FAO/HWSD (Nachtergaele et al. 2009). Data represents number of 3 second pixels within each 30second grid cell in each of 8 slope classes.

Conceptually, the 3-second slope pixels are allocated throughout the 30 second grid cell subject to only one constraint: flatter slope pixels classes are allocated preferentially to agricultural classes.

Example
A 30 arc-second pixel is 33% agriculture and has:

- 5% area in the 0-2 degree slope class
- 20% area in the 2-5 degree slope class
- 30% area in the 5-10 degree slope class
- 10% area in the 10-15 degree slope class
- 10% area in the 15-20 degree slope class
- 25% area in the 25-50 degree slope class

The algorithm assigns the agriculture as follows:

- 5% on 0-2 degree
- 20% on 2-5 degree
- 8% on 5-10 degree

Appendix C: Land degradation

This section describes the preliminary work to quantify the effects of land degradation on crop yields, and thus land value. It has four subsections: (1) overview of the range of extent and location of degraded lands among existing map data products, (2) summary of previous research that estimates the cost of land degradation on crop production and human wellbeing, (3) challenges of using indicators to quantify degraded lands, and (4) methods for quantifying and mapping three indicators of land degradation—soil erosion, water availability, and salinity—known to limit yield. The fourth subsection will also include our literature review of the relationships between indicators of degradation and crop yields.

We also produce global maps of three indicators of degraded land and estimates of yield reduction from land degradation.

Overview

1. Land degradation poses a major risk for both near- and long-term food production.

In addition to food production, land degradation decreases many other ecosystem services that affect human wellbeing, such as clean water (Potts et al. 2018). Despite widespread knowledge, land degradation and its impact on production is very difficult to measure across broad areas as many characteristics of soil health can't be measured by satellites. Of the major data sets, global estimates of total degraded land area range from 1 billion to 6 billion hectares, and the regional distribution differs just as widely (Gibbs and Salmon 2015). The estimates vary due to (1) definitions, such as conversion of natural land vs. soil health characteristics that affect agricultural productivity; (2) types of indicators, such as normalized difference vegetation index vs. bare soil, (3) number of indicators (one vs. many vs. composite), and (4) methods, such as remote sensing vs. expert opinion. Despite the range of estimates of the extent and precise location of degraded lands, dryland regions are typically more degraded, especially when the natural ecosystem has low productivity, the climate is highly variable, and where there is a dense or rapidly expanding population of marginalized people (Potts et al. 2018).

2. The cost of land degradation and its impacts on crop production and human wellbeing

Much like the challenge of mapping the extent and location of degraded lands, it is equally (or more) challenging to quantify the financial cost of degraded land. A recent study estimated the Total Economic Value (TEV) of land degradation at $231B, or 0.41% of GDP (in 2007 USD) (Nkonya et al. 2016). Only 46% of the total costs affect local conditions only, as TEV accounts for ecosystem services, such as carbon sequestration and cultural services, which provide benefits beyond their immediate area (Nkonya et al. 2016). Other estimates of the cost of land degradation range from $17.6B to $9.4T (a review of 12 studies reported in Nkonya et a. 2016).

Most efforts to quantify the impact of land degradation on food production focus on crop yields. For example, one study estimates that 40% of agricultural land is degraded to the point at which

yields are severely reduced, and another 9% is no longer suitable for crop production at all (Bossio et al. 2010). Another recent study by IFPRI (Nkonya et al. 2016) estimates that cost of "soil mining" (depleting the soil of nutrients) for corn, wheat, and rice production is about $56.6B/year or 0.10% of global GDP (in 2007 dollars).

These impacts of land degradation can lead to increased inequality, as access to natural resources tends to impact poor communities more than wealthy ones (Barier 2010, Dasgupta and Maler 1996, Perrings 2014). This relationship is particularly true where agriculture is a primary source of income for the poor in lower income countries, where the impact of soil loss from land degradation has reduced as much as 5% of national GDP (Potts et al. 2018).

3. Indicators of degraded land: challenges and a path forward

There are several indicators of degraded lands that are used for broader assessments, such as the SDG target 15.3, UNCCD (Orr 2011), and GLADA (Nachtergaele and Licona-Manzur 2008), which have 3, 11, and 132 indicators, respectively. However, there are several challenges to using these indicators for measuring degradation and its impact. First, many of the indicators are difficult to (or not amenable) quantify. Second, many of the indicators are multi-metric. While these multi-metric indicators aim to quantify complex attributes, such as "sustainability" or "ecological integrity," they create a false impression that the relationships among several factors are known and that what defines degraded is consistent across geographies and farming system type. Third, degraded is a value relative to a baseline condition. Many areas were degraded before the satellite record (Gibbs and Salmon 2015), which can result in stable areas being interpreted as not degraded. Related, the baseline needs to be defined (Prince 2016)—such as natural, historical, current, etc.—making it difficult to compare among assessments. Fourth, the impacts of degradation on food production and human wellbeing can be "hidden" or mitigated. For example, farming practices (e.g., fertilizer, seed quality) can mitigate against degraded conditions. Land degradation impact on health can be mediated by household assets, social networks, and institutions (Myers et al 2013).

Another consideration in modeling yield impacts of land degradation is that land degradation is impacting current yields, so applying a factor for yield degradation to a near-future yield time-series risks double-counting degradation impacts.

Due to these challenges, we do not incorporate indicators of degraded land into the yield model for this project. Rather, we use published relationships between land degradation factors and yield decrease, and then apply a *post hoc* factor to decrease **yield ceilings** based on analysis of intensity of land degradation.

In this CWON project, we are ignoring possible correlations among factors. Thus, we are developing a framework for a first-order assessment of the impacts of land degradation on crop yields. Further, this approach is more transparent, enabling impact assessments as new valuation methods are developed.

4. Methods for quantifying and mapping indicators of land degradation and their impact on crop yields.

Soil erosion risk

Soil erosion risk was calculated using the Revised Universal Soil Loss Equation (RUSLE2015) model. Since we are interested in potential erosion, the crop type and management practices are not included as they are local modifiers that will change. More specifically, soil erosion potential is calculated as follows:

$$A = R * K * LS$$

Where,
A is the average potential soil loss (tons/ha)
R is the Rainfall erosivity factor
K is the erosivity factor of the soil type, and
LS is the slope length * slope steepness

Rather than develop a new global data set of potential soil erosion, we used a product developed by Borrelli et al. (2017) (Figure 1). Borrelli and colleagues estimated soil erosion (tons/hectare/year) at 250m resolution for the years 2001 and 2012. The only difference between the two estimates was changes in the amount and location of agricultural lands. Since physical properties influencing erosion, such as slope length and steepness, are assumed to be stable, we use the 2012 data. The bigger limitation of the data set is that the only publicly available version of these data has been resampled to 5-minute resolution (~10km). We have requested the finer scale data from the authors but have not received a response.

Figure 1

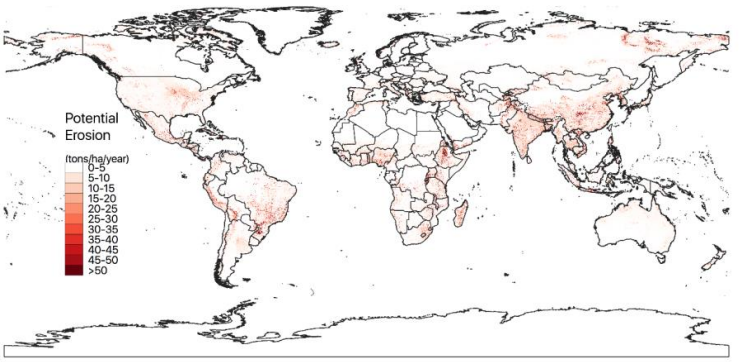

We used the following rules to estimate yield losses from the map of soil erosion from Borelli et al (2017):

- No yield loss when potential soil erosion is <2 tons/ha/year
- Yields are reduced when soil erosion is >2 but less than 25 tons/ha/yr[2] by:
    - 0.02% in North America and Western Europe (den Biggelaar et al. 2003)
    - 0.04% in the rest of the World (den Biggelaar et al. 2003)
- Yields are reduced by 3% when soil erosion is > 25 tons/ha/yr (Pierce et al. 1983).[3]

Figure 2

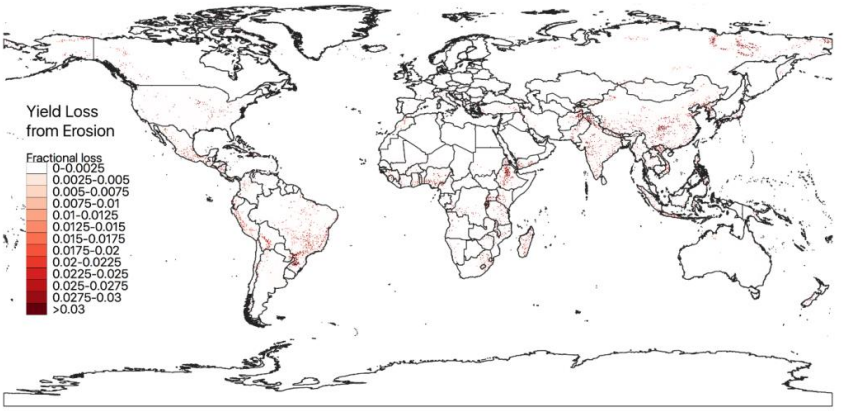

Recommendations for future work:

Finer resolution. Estimates of soil erosion, and hence yield losses, could be improved if this analysis were completed at a finer resolution. The potential soil product we used here was a 5-minute (~10km) resolution (Borrelli et al. 2017). Since the original product was developed at 250m resolution before rescaling to a coarser resolution, the main limitation of using the 5-minute data set for future scenarios would be the slope length and steepness factors, which will likely vary more than the rainfall erosivity factor. Although soils will vary within a 10km area,

[2] We added the bounds of >2 but <25 tons/ha/yr soil loss as we had sources for fractional yield estimates above and below that range. The values within this range were yield loss estimates were from den Biggelaar et al. (2003), which provided estimates without thresholds of soil loss.

[3] Pierce et al. 1983 estimated 2-4% productivity loss when severe erosion, which they defined as >25 t/ha/yr. Here we used the middle of the range (3%).

the soils data for many parts of the world are very coarse, thus finer resolution soils data would have less effect on the soil erosion estimates.

Sensitivity analysis for the rainfall erosivity factor. The rainfall erosivity factor (R)—the power of rainfall to create erosion from water—is difficult to quantify in the absence of long-term, sub-daily rainfall data. As a result, it is difficult to estimate R in many places in the world. A simple sensitivity analysis would be to model soil erosion of over a range R values, such as +10%, -10%, etc. *In addition to sensitivity analysis for estimating soil erosion under current average conditions, such analysis would provide a better sense of erosion during extreme events. It could also inform how erosion may change in projected climate scenarios from the IPCC.* (The IPCC scenarios will not provide estimates of sub-daily variability so a simpler approach for estimated changes would be needed and more transparent.) Further work could be done to compare R values using different climate reanalysis products, although this would be very time intensive and would likely not be more helpful than a simple sensitivity analysis described above as the products have a very coarse spatial scale.

Future landcover scenarios. The analysis could be extended to include future landcover scenarios, such as agricultural expansion. This would be fairly straightforward since the rainfall erosivity index (R), inherent erosivity of soil type (K), and slope length * steepness (LS) would be the same. The only input that would change would be the extent of agriculture. In other words, these scenarios would not change the potential soil erosion, but would change estimates of current and future erosion as landcover changes.

Soil salinity and salinization risk

Moderate and high levels limit both germination and plant growth, by both toxicity and reducing the ability of roots to uptake water. Salt concentration can be naturally high. Salinization—or increased salinity—can increase through weathering of bedrock, wind deposition, salt water intrusion from the ocean, and irrigation. Irrigation can increase salinity in areas where surface or groundwater with high salt content is applied to the soils. The impacts of irrigation can be mitigated by excess irrigation to "flush" salt buildup beyond the crop's root zone.

We used the Harmonized World Soils Database's excess salt in soils product (Fisher et al. 2008), which mapped four categories of limitations to plant growth (Figure 3), to estimate yield reductions from excess salts.

Figure 3

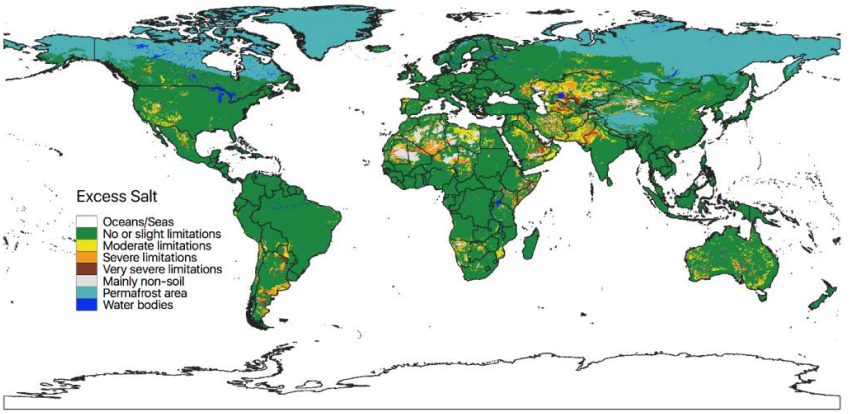

The following rules were used to estimate yield losses from soil salinity:

- Yields are not reduced for Category 1 soils
- Yields are reduced by 30% for Category 2 soils[4]
- Yields are reduced by 50% for Category 3 soils
- Yields are reduced by 70% for Category 4 soils

The changes in yields were then calculated for 10 crops using the above rules and yield data from Ray et al. 2019. Figure 4 shows the fractional yield loss from soil salinity.

[4] Fisher et al. 2008, provide ranges of limitations for each category. We used the mid-point for Categories 2 and 3. For example, Category 2 has a range of limiting growth potential to 60-80% so we assumed 70% of the potential, which corresponds to a 30% reduction. For Category 4, defined as limiting growth to <40%, we assumed at 70% reduction in yields.

Figure 4

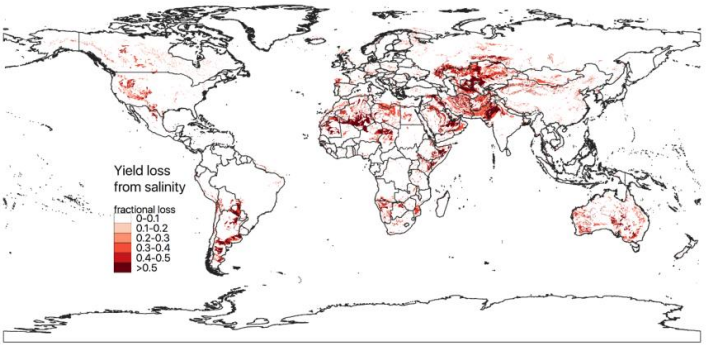

To assess risk of salinization, we identified areas where irrigation is used on saline soils. These areas were defined as places that are equipped for irrigation (Siebert et al. 2013) and the soil salinity limits plant growth (Limitation Categories 2-4 in Fisher et al. 2008). Figure 5 maps these higher risk areas.

Figure 5

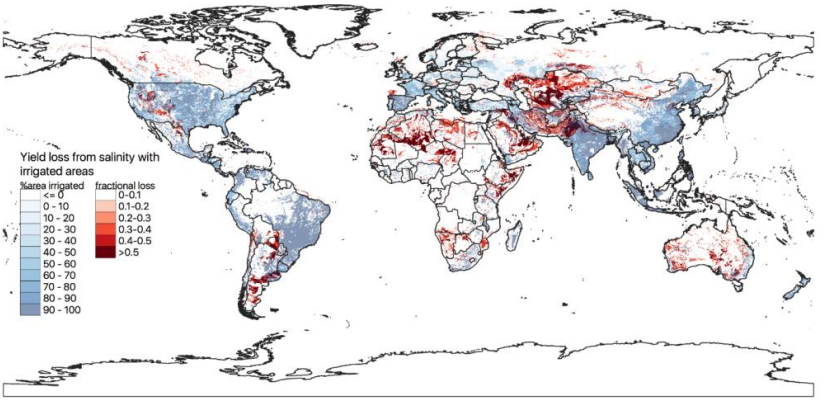

Water availability risk

Approximately 70% of all of humanity's water use is for agriculture (Gleick et al. 2009). Unfortunately, source water is being depleted as consumption outpaces recharge (Wada et al. 2010, Wada et al. 2013, Gleeson et al. 2012, Brauman et al. 2016). Our aim here was to assess and map risk (Figure 6). We then estimated the yield loss (for 10 crops) if irrigated areas needed to switch to rainfed agriculture (Figure 7). It was not possible to further assess potential yield losses from water availability risk as there are not pre-defined relationships here as there is for soil erosion and salinity reported above.

We used the water depletion index (categorical data) from Brauman et al. 2016:

- High[5] = 75-100% and 100+%
- Medium = Seasonal (at least 1 month > 75%)

Figure 6. Water availability risk from Brauman et al. 2016

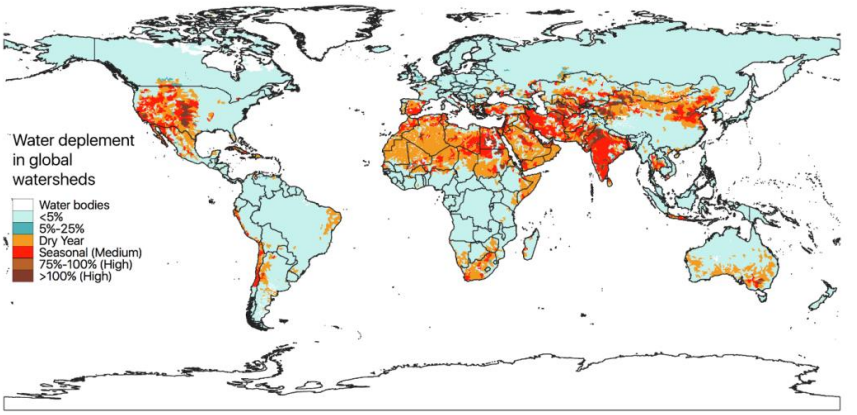

[5] We aggregated categories into High and Medium

Figure 7. Fractional yield loss from switching from irrigated to rainfed agriculture in unsustainably irrigated areas for the example of wheat.

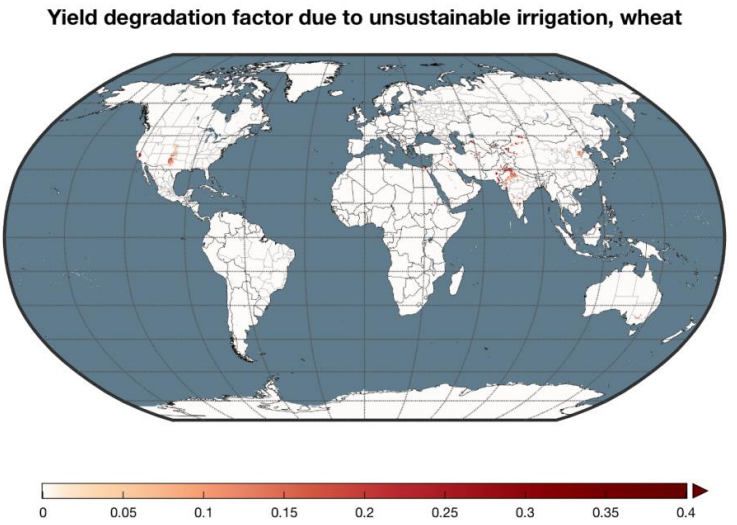

Note: Analysis was completed for 10 crops and is limited to those areas currently irrigated. The above example is wheat.

Algorithmic approach to calculating land degradation inputs

Three independent map layers of land degradation potential at 5 minute resolution are calculated, corresponding to erosion, salinization, and loss of ground water for irrigation (see preceding sections for description of calculation of these layers.) These layers are valued in percentage of yield lost in a degradation situation. These are combined into a governing land degradation factor F with a "law of the minimum" approach, in which the degradation factor causing the greatest loss of yield is the only one considered at each pixel.

For each crop and country combination, the calculated yield ceiling (see appendix A) is decreased by a factor η calculated as a weighted average as follows:

$$\eta = \frac{\sum Fya}{\sum ya}$$

Where F is the governing land degradation yield loss factor, y is pixel-level yield, and a is pixel-level harvested area.

References:

Barbier, E. B., & Hochard, J. P. (2016). Does Land Degradation Increase Poverty in Developing Countries? *PLOS ONE*, *11*(5), e0152973. https://doi.org/10.1371/journal.pone.0152973

Bossio, D., Geheb, K., & Critchley, W. (2010). Managing water by managing land: Addressing land degradation to improve water productivity and rural livelihoods. *Agricultural Water Management*, *97*(4), 536 – 542.

Brauman KA, Richter BD, Postel S, Malsy M, Flörke M. 2016. Water depletion: An improved metric for incorporating seasonal and dry-year water scarcity into water risk assessments. *Elem Sci Anthr* 4(0):000083. http://www.elementascience.org/articles/10.12952/journal.elementa.000083

Dasgupta, P., & Mäler, K.-G. (1996). Environmental economics in poor countries: the current state and a programme for improvement. *Environment and Development Economics*, *1*(1), 3 – 7.

den Biggelaar, C., Lal, R., Eswaran, H., Breneman, V. E., & Reich, P. F. (2003). Crop yield losses to soil erosion at regional and global scales: evidence from plot-level and GIS data. In K. Wiebe (Ed.), Land Quality, Agricultural Productivity, and Food security. Cheltenham, U.K.: Edward Elgar.

Evenson RE, Fuglie KO. 2010. Technology capital: the price of admission to the growth club. *J Product Anal* [Internet]. 33(3):173–90. http://link.springer.com/10.1007/s11123-009-0149-3

FAO & ITPS. (2015). *Status of the World's Soil Resources (SWSR) – Main Report*. Food and Agriculture Organization of the United Nations and Intergovernmental Technical Panel on Soils, Rome, Italy.

Fick SE, Hijmans RJ. 2017. WorldClim 2: new 1-km spatial resolution climate surfaces for global land areas. *Int J Climatol.* 37(12):4302–15. http://doi.wiley.com/10.1002/joc.5086

Fischer, G, F Nachtergaele, S Prieler, H T van Velthuizen, L Verelst, and D Wiberg. "Global Agro-Ecological Zones Assessment For Agriculture (GAEZ 2008)." Laxenburg, Austria and FAO, Rome, Italy: IIASA, 2008. http://www.fao.org/soils-portal/soil-survey/soil-maps-and-databases/harmonized-world-soil-database-v12/en/.

Ganasri, B. P., & Ramesh, H. (2016). Assessment of soil erosion by RUSLE model using remote sensing and GIS - A case study of Nethravathi Basin. *Geoscience Frontiers*, *7*(6), 953–961. https://doi.org/10.1016/j.gsf.2015.10.007

Gerber et al. [in prep]. Room to grow: trends in yield gaps indicate future yield stagnation.

Gibbs, H. K., & Salmon, J. M. (2015). Mapping the world's degraded lands. Applied Geography, 57, 12–21. https://doi.org/http://dx.doi.org/10.1016/j.apgeog.2014.11.024

Gleeson, T. et al., 2012. Water balance of global aquifers revealed by groundwater footprint. *Nature*, 488(7410), pp.197–200. Available at: http://dx.doi.org/10.1038/nature11295

Gleick, P. H., Cooley, H. & Morikawa, M. 2009. The World's Water 2008-2009: the biennial report on freshwater resources. Island Press.

Hengl, T. et al., 2017. SoilGrids250m: Global gridded soil information based on machine learning B. Bond-Lamberty, ed. *PLOS ONE*, 12(2), p.e0169748. Available at: https://dx.plos.org/10.1371/journal.pone.0169748

Hijmans, R.J., S.E. Cameron, J.L. Parra, P.G. Jones and A. Jarvis, 2005. Very high resolution interpolated climate surfaces for global land areas. International Journal of Climatology 25: 1965-1978.

Mueller ND, JS Gerber, DK Ray, N Ramankutty, JA Foley. 2012. Closing yield gaps: Nutrient and water management to boost crop production. *Nature*, doi:10.1038/nature.2012.11306.

Myers, S. S., Gaf, L., Golden, C. D., Ostfeld, R. S., & Redford, K. H. (2013). Human health impacts of ecosystem alteration. *Proceedings of the National Academy of Sciences of the United States of America*, *110*(47), 18753 – 18760.

Nachtergaele, F. O., Petri, M., Biancalani, R., Lynden, G. van, Velthuizen, H. van, & Bloise, M. (2011). *Global Land Degradation Information System (GLADIS). An Information database for Land Degradation Assessment at Global Level*. Technical working paper of the LADA FAO / UNEP Project.

Nachtergaele, F, van Velthuizen, H., Verelst, L., Batjes, N. et al. 2008. *Harmonized World Soil Database*.

Neitsch, S. L., Arnold, J. G., Kiniry, J. R., & Williams, J. R. (2005). *Soil and Water Assessment Tool - theoretical documentation*. Temple - Texas: Blackland Reserach Center.

Nkonya, E., Anderson, W., Kato, E., Koo, J., Mirzabaev, A., Braun, J. Von, & Meyer, S. (2016a). Global Cost of Land Degradation. In E. Nkonya, A. Mirzabaev, & J. von Braun (Eds.) *Economics of land degradation and improvement: A global assessment for sustainable development* (pp. 117 – 166). Cham, Switzerland: Springer International Publishing.

Oldfield, E.E., Bradford, M.A. & Wood, S.A., 2019. Global meta-analysis of the relationship between soil organic matter and crop yields. *SOIL*, 5(1), pp.15–32. Available at: https://www.soil-journal.net/5/15/2019/

Oliveira, A. H., Silva, M. A. da, Silva, M. L. N., Curi, N., Neto, G. K., & Freitas, D. A. F. de. (2013). Development of Topographic Factor Modeling for Application in Soil Erosion Models. In *Soil Processes and Current Trends in Quality Assessment*. InTech. https://doi.org/10.5772/54439

Orr, B. J. (2011). Scientific review of the UNCCD provisionally accepted set of impact indicators to measure the implementation of strategic objectives 1, 2 and 3: White Paper – Version 1 04. Tucson, Arizona, USA. Retrieved from http://www.unccd.int/en/programmes/Science/Monitoring- Assessment/Documents/White paper_Scientific review set of indicators_Ver1.pdf

Panagos, P., Borrelli, P., Meusburger, K., Yu, B., Klik, A., Lim, K. J., … Ballabio, C. (2017). Global rainfall erosivity assessment based on high-temporal resolution rainfall records. *Scientific Reports*, *7*(1), 1–12. https://doi.org/10.1038/s41598-017-04282-8

Perrings, C. (2014). Environment and development economics 20 years on. *Environment and Development Economics*, *19*(3), 333 – 366.

Portmann FT, Siebert S, Doll P. 2010. MIRCA2000: global monthly irrigated and rainfed crop areas around the year 2000: a new high-resolution data set for agricultural and hydrological modeling. *Global Biogeochem Cycles* 24(1):GB1011. http://dx.doi.org/10.1029/2008GB003435

Potts, M. D., Holland, T., Erasmus, B. F. N., Arnhold, et al. Chapter 5: Land degradation and restoration associated with changes in ecosystem services and functions, and human well-being and good quality of life. In *IPBES (2018): The IPBES assessment report on land degradation and restoration.* Montanarella, L., Scholes, R., and Brainich, A. (eds.). Secretariat of the Intergovernmental Science-Policy Platform on Biodiversity and Ecosystem services, Bonn, Germany.

Prince, S. D. (2016). Where Does Desertification Occur? Mapping Dryland Degradation at Regional to Global Scales. In R. Behnke & M. Mortimore (Eds.), The End of Desertification? Disputing Environmental Change in the Drylands. (pp. 225–263). Berlin Heidelberg: Springer Earth System Science. https://doi.org/10.1007/978-3-642-16014-1_9

Qadir, M., Quillérou, E., Nangia, V., Murtaza, G., Singh, M., Thomas, R. J., et al. (2014). Economics of salt-induced land degradation and restoration. *Natural Resources Forum*, *38*(4), 282–295. http://doi.org/10.1111/1477-8947.12054

Ray, DK, PC West, M Clark, JS Gerber, AV Prishchepov, S Chatterjee. 2019. Climate change likely already affects global food production. *PLOS ONE*. doi: 10.1371/journal.pone.0217148

Siebert, S, Henrich,V., Frenken, K., and Burke, J. (2013). Global Map of Irrigation Areas version 5. Rheinische Friedrich-Wilhelms-University, Bonn, Germany / Food and Agriculture Organization of the United Nations, Rome, Italy

Stoorvogel, J. J., Bakkenes, M., ten Brink, B. J. E., & Temme, A. J. A. M. (2017). To What Extent Did We Change Our Soils? A Global Comparison of Natural and Current Conditions. *Land Degradation and Development*, *28*(7), 1982–1991. https://doi.org/10.1002/ldr.2721

Wada, Y. et al., 2010. Global depletion of groundwater resources. *Geophysical Research Letters*, 37(20), p.n/a-n/a. Available at: http://doi.wiley.com/10.1029/2010GL044571

Wada, Y. et al., 2013. Human water consumption intensifies hydrological drought worldwide. *Environmental Research Letters*, 8(3), p.034036. Available at: http://iopscience.iop.org/1748-9326/8/3/034036/article/

Weedon GP, Balsamo G, Bellouin N, Gomes S, Best MJ, Viterbo P. 2014. The WFDEI meteorological forcing data set: WATCH Forcing Data methodology applied to ERA-Interim reanalysis data. *Water Resour Res* 50(9):7505–14. http://doi.wiley.com/10.1002/2014WR015638

West, P.C., Gerber, J.S., Engstrom, P.E., Mueller N.D. et al., 2014. Leverage points for improving global food security and the environment. *Science*, 345(6194), pp.325–328. Available at: http://www.sciencemag.org/content/345/6194/325.abstract

Wicke, B., Smeets, E., Dornburg, V., Vashev, B., Gaiser, T., Turkenburg, W., & Faaij, A. (2011). The global technical and economic potential of bioenergy from salt-affected soils. *Energy & Environmental Science*, *4*(8), 2669–13. http://doi.org/10.1039/c1ee01029h

Appendix D: Crop area under future scenarios

The initially proposed method to calculate future area was found to lead to unrealistic outcomes. These outcomes arose because the future scenarios were determined by an integrated assessment model used by the global futures project, and those scenarios had significant decreases in cropland in some future scenarios.

For example, New Zealand has 607 kHa of cultivated land in 2015 (according to the ESA-LCC satellite product) but in future scenarios has 868 kHa (SSP1) 518 kHa (SSP2) and 4295 kHa (SSP3).

As annexes to this report, we provide files with country-specific area for each of the three SSPs (Shares Socioeconomic Pathways), with columns for country code, country name, ESA 2015 crop area, GFP/IAM 2050 crop area, estimate of total of arable land calculated with a biophysical suitability model used in GFP (but independent of SSPs), and FAO's reported arable land in 2018.

File names:
`TableOfArableLand_SSP1.csv`
`TableOfArableLand_SSP2.csv`
`TableOfArableLand_SSP3.csv`

Appendix E: Calculations of Producer Prices

A bulk download of "Value of Agricultural Production Data" was downloaded from FAOSTAT on Sep 21, 2019. This data had last been updated by FAO on Nov 30, 2018. As of September 15, 2020, this was the latest data revision available. Data was only available through 2016.

Value of Agricultural Production is reported in various ways, including:

Gross Production Value (constant 2014-2016 1000 I$)
Gross Production Value (current million US$)
Gross Production Value (constant 2014-2016 million US$)

For all calculations presented in this report and associated tables, GPV in constant US$ was used for reporting and normalization where possible. However, there were some cases (e.g. Afghanistan) where no data was available in constant US$. In these cases, constant international dollars were used. There were some cases (e.g. Iraq) where some crops were given values only in constant US$ and some crops were given values only in constant international dollars. In these cases, crop-specific weights were normalized as in equation E1.

$\gamma_{c,t}^{y} = \left(\frac{1}{GVP_{US\$}}\right) \sum_{k=1}^{M} \gamma_{c,k,t}^{y} \times {p_{c,k,t;VE} q_{c,k,t}} \Big/ {GVP_{c,t}^{C10}} + \left(\frac{1}{GVP_{I\$}}\right) \sum_{k=1}^{N} \gamma_{c,k,t}^{y} \times {p_{c,k,t;VE} q_{c,k,t}} \Big/ {GVP_{c,t}^{C10}}$ Where the first sum is over crops denominated with constant USD and the second sum is over crops denominated in constant International Dollars. The subscript VE refers to Value Element (USD or International Dollars) $GVP_{c,t}^{C10}$ is the sum of production across the 10 crops, k=1…10: $$GVP_{c,t}^{C10} = \sum_{k=1}^{10} \left(\frac{p_{c,k,t;VE}}{GVP_{VE}}\right) p_{c,k,t} \times q_{c,k,t}$$ And $GVP_{US\$}$ is total value of agricultural production in US$, $GVP_{I\$}$ is Total value of agricultural production in I$, and $p_{US\$;c,k,t}$ is agricultural production value for county c, crop k, year t in constant US$, and $p_{I\$;c,k,t}$ is agricultural production value for county c, crop k, year t in constant international. Note that $p_{US\$;c,k,t} = p_{c,k,t}$ (i.e. when currency subscript implicit, it refers to constant USD.)	Equation E1

Appendix F: Proposed future improvements

If yield trend negative, current methods allow yield to decrease eventually to zero. Possible modifications that may be more in line with expectations: (1) replace with mean yield of last 10 years so that yields never go to zero; (2) start to decrease area assigned to that crop – presumably yields heading to zero reflect changes which would result in less harvested area.

Perturbation method for other crops. While this would require a substantial research effort (would need to use satellite data and likely some machine learning methods to allocate reported growth in area and yield at a subnational level) the resulting dataset could be extremely beneficial to calculations of CWON.

See Appendix C: Land degradation for additional areas of improvement

In CWON work, the factor alpha is constant. It has been noted by Madhur Gautam (World Bank) that this approximation will break down as yield gaps close, or all available land is converted to agriculture. Future work could model these changes in alpha and incorporate.

Appendix G: Description of datafiles

See 'DescriptionOfColumnsInDataFiles.docx'